PRODUCTION OF GREEN GASOLINE AND LIGHT OLEFINS BY CRACKING OF TRIGLYCERIDE-RICH BIOMASS OVER NANO-ZSM-5/SBA-15 ANALOG COMPOSITES WITH VARIABLE Si/Al RATIOS

Vu Xuan Hoan[1], Nguyen Sura[1], Dang Thanh Tung[1], Phan Minh Quoc Binh[1], Nguyen Anh Duc[1]
Michael Hunger[2], Udo Armbruster[3], Andreas Martin[3]
[1]*Vietnam Petroleum Institute*
[2]*The University of Stuttgart*
[3]*Leibniz Institute for Catalysis*
Email: hoanvx.epc@vpi.pvn.vn

Summary

Nano-ZSM-5/SBA-15 analog composites (ZSC) with different Si/Al molar ratios were prepared and their performance was evaluated in catalytic cracking of triglyceride-rich biomass. It was found that the initial Si/Al ratio used in the synthesis mixture significantly affects the physicochemical properties and consequent catalytic performance of ZSC catalysts. Increasing the initial Si/Al ratio raises the content of nano-ZSM-5 phase at the expense of SBA-15 analog phase. The total acidity enhances with the fraction of nano-ZSM-5 phase despite the decreased amount of incorporated aluminum as the Si/Al ratio varies from 10 to 30. However, the total acidity decreases when raising the Si/Al ratio to 50 because the low incorporated aluminium has not been compensated by the increased nano-ZSM-5 phase. The catalytic performance of ZSC catalysts with variable Si/Al ratios was evaluated in the catalytic cracking of waste cooking oil as a real feedstock. The results showed that the sufficient amount of nano-ZSM-5 phase obtained by properly tuning the initial Si/Al ratio is of crucial importance to achieve the superior catalytic performance of ZSC catalysts in catalytic cracking of triglyceride-rich biomass.

Key words: *Nano-ZSM-5, SBA-15 analog, Si/Al ratio, green gasoline, light olefins.*

1. Introduction

The processing of biomass, particularly triglyceride-rich biomass, by catalytic cracking represents a promising alternative for the production of green fuels and chemicals. This strategy allows rapid transition to a more sustainable economy without large capital investments for new reaction equipment by utilising the existing infrastructure of petroleum refineries [1, 2]. However, biomass derived feedstocks are chemically different from petroleum feedstocks; therefore, the development of suitable catalysts is required for efficient conversion of triglyceride-rich biomass.

There is a rich body of literature on catalytic cracking of triglyceride-based feedstocks in which various cracking catalysts have been investigated [1 - 3]. It has shown that the catalyst performance is mainly governed by acidity, pore size and shape. Active alumina, alumina-silica, MCM-41 or SBA-15 type materials usually give a lower gas yield and higher coke formation due to their low acidity and lack of shape selectivity [3, 4]. Compared to these amorphous materials, crystalline zeolites such as ZSM-5, Y or Beta are superior, producing more desirable products, i.e. gasoline and light olefins because they have strong acidity and uniform micropores of molecular dimensions which generate shape selectivity [3 - 6]. Among zeolite-based catalysts, the medium-pore zeolite ZSM-5 stands out as the most effective zeolite type catalyst for conversion of triglycerides to gasoline-range hydrocarbons [5, 6]. Unfortunately, conventional ZSM-5 zeolites generally yield large fractions of undesired gaseous products with low concentrations of C_2-C_4 olefins. Hence, many attempts have been focused on modifications of ZSM-5 zeolites to enhance the selectivity of light olefins. Reducing the amount of acid sites by impregnation with potassium [7] hindered secondary cracking reactions, leading to the increased fractions of liquid products and light olefins, but the decreased fractions of gaseous products. Botas et al. [8] showed that nanocrystalline and hierarchical ZSM-5 catalysts indeed produced more light olefins than conventional ZSM-5 because of their ability to prevent the primary light olefins from further transformation thanks to shortened diffusion path lengths. Recently, we reported a highly selective catalyst, denoted as nano-ZSM-5/SBA-15 analog composite (ZSC) for conversion of triglyceride-rich biomass toward light olefins. The selectivity

to C_2-C_4 olefins is remarkably high (> 90%) regardless of cracking severity and feedstock composition [9].

In this study, we explore the influence of the Si/Al ratio on the catalytic performance of ZSC catalysts in catalytic cracking of triglyceride-rich biomass. It has been reported that the Si/Al ratio is an important factor affecting the physicochemical properties and consequent catalytic performance of ZSM-5 based catalysts in various reactions such as alkane dehydrogenations [10] or cracking of C_4 alkanes [11]. However, the effect of the Si/Al ratio on the performance of ZSM-5 based catalysts in catalytic cracking of triglyceride-rich biomass is scarcely described in the literature.

2. Experimental

2.1. Chemicals

The chemicals used in this study were tetraethyl orthosilicate (TEOS, 99%, Aldrich), tetrapropylammonium hydroxide (TPAOH, 20% in water, Aldrich), aluminum isopropoxide (AIP, 98%, Aldrich), triblock copolymer pluronic P123 (EO20PO70EO20, MW = 5800, Aldrich), hydrochloric acid (HCl, 37%, J.T.Baker) and ammonium hydroxide (NH_4OH, 25%, Acros).

2.2. Synthesis

The preparation of nano-ZSM-5/SBA-15 analogs from ZSM-5 nanoseeds involves a two-step process, being similar to that of the previous work [12]. In the first step, 6.0g of TEOS, 10.0g of TPAOH, 2.0g of distilled H_2O were mixed at room temperature and stirred overnight for complete hydrolysis. Then the amounts of AIP required to obtain the Si/Al molar ratio in the range of 10 - 50 were added and stirred for 24 hours, followed by pre-crystallisation at 90°C for 24 hours in a reflux system to yield the desired precursor solutions.

In the second step, the P123 solution was prepared by dissolving 2.0g of P123 in 75ml of 1.6M HCl at room temperature for 4 hours to get a clear solution. Then, the precursor solution prepared as described above was added dropwise to the P123 solution, followed by aging at 40°C for 24 hours to convert unreacted precursors to ordered mesoporous SBA-15 analogs in strongly acidic media. Before transferring the mixture into a Teflon-lined autoclave for hydrothermal treatment at 200°C for 24 hours, the pH value was adjusted to 3.5 with an aqueous NH_3 solution. The final product was filtered off, washed with distilled water, and dried at 100°C for 12 hours. The as-synthesised material was calcined in air at 550°C for 5 hours with a heating rate of 2K/min to remove the organic template. The calcined solid was transformed into the protonated form by two consecutive exchanges in 0.5M NH_4NO_3 solution at 80°C for 4 hours. The obtained catalysts are denoted as ZSC-SAx, where ZSC represents the nanosized ZSM-5/SBA-15 analog composite; x is the initial Si/Al (SA) molar ratio in the gel mixture.

2.3. Characterisation

SAXS measurements were carried out using a Kratky-type instrument (SAXSess, Anton Paar, Austria) operated at 40kV and 50mA in slit collimation using a two-dimensional CCD detector. X-ray diffraction (XRD) measurements were carried out on a theta/theta diffractometer (X'Pert Pro from Panalytical, Almelo, Netherlands) with CuKα radiation (λ = 0.15418nm; 40kV, 40mA) and an X'Celerator RTMS Detector. Nitrogen physisorption measurements were carried out at -196°C on an ASAP 2010 Micromeritics apparatus. The BET specific surface area was calculated using adsorption data at a relative pressure (p/p_0) of 0.05 - 0.25, and the total pore volume was estimated from the amount adsorbed at a relative pressure of about 0.976. NH_3-TPD experiments were carried out in a quartz tube reactor in the range of 100 - 550°C. The liberated ammonia was continuously detected by a thermal conductivity detector (TCD, Gow-Mac Instrument Co.). The Al and Si contents were determined by ICP-AES (715-ES, Varian) and AAS (Analyst 300, Perkin Elmer), respectively. For this purpose, the samples were digested with a mixture of HCl-HNO_3-HF in a microwave-assisted sample preparation system (Multi wave, Anton Paar/Perkin-Elmer) at 200°C and 60bars. The solid-state NMR investigations were performed with the hydrated material using a Bruker BioSpin Avance III 400WB spectrometer at the resonance frequency of 104.3 MHz for ^{27}Al nuclei. More details of these characterisation methods are described elsewhere [12].

2.4. Catalytic test experiments

The catalytic cracking of waste cooking oil (WCO) was performed on a fully automated Single Receiver Short-Contact-Time Microactivity Test unit (SR-SCT-MAT, Grace Davison). The utilisation of WCO as a potential triglyceride-rich biomass for production of green fuels and chemicals is preferred because it does not compete with food crops and arable land. Details of the experimental setup, testing conditions, feedstock and product analyses are given in the previous work [9].

In a typical run, 1.75g of WCO was fed into the reactor which contained a desired amount of catalyst diluted with glass beads to maintain a constant-volume reaction. The cracking reaction was carried out at ambient pressure, 550°C, the catalyst-to-oil (CTO) mass ratio of 0.4 ($g \cdot g^{-1}$) and a reaction time of 12s. After the reaction, stripping of the catalyst was done by using a nitrogen purge. The gaseous and liquid products were collected in the single receiver cooled to 18°C via an external cooling system. All catalytic test experiments were repeated at least two times to check the reproducibility, and mass balances in all runs were between 95 and 100% of the injected feed.

The products comprised mainly hydrocarbons along with oxygenated compounds (water, CO and CO_2) and coke. The gaseous hydrocarbon fraction was divided into dry gas (hydrogen, methane, ethane, and ethene) and liquefied petroleum gas (LPG, propane, propene, butenes and butanes). The liquid hydrocarbons were lumped in terms of boiling ranges: C_{5+} gasoline (< 221°C), light cycle oil (LCO; 221 - 360°C) and heavy cycle oil (HCO; > 360°C).

The gaseous products were analysed according to the ASTM D1945-3 method using a Refinery Gas Analyser (Agilent 7890A). The liquid organic products were classified according to the boiling ranges: C_{5+} gasoline, LCO and HCO as mentioned above by means of simulated distillation (ASTM D2887) on a Simulated Distillation Gas Chromatograph (Agilent 7890A). Water content was measured by Karl Fischer titration (MKS-520, Kem) and coke amount on the spent catalyst was determined by an elemental analyser (CS600, Leco).

The yield toward different products (Y_i, wt%) is defined as gram of product i per gram of the feed. The standard MAT conversion is defined as 100% - ($Y_{HCO} + Y_{LCO}$). The selectivity to C_2-C_4 olefins (light olefins) is defined as the fraction of C_2-C_4 olefins per total fraction of C_2-C_4 hydrocarbons.

3. Results and discussion

3.1. Physicochemical properties of ZSC catalysts with variable Si/Al ratios

Figure 1 depicts the small angle X-ray scattering (SAXS) patterns of ZSC materials prepared from ZSM-5 precursors with the different initial Si/Al ratios. It can be seen that samples ZSC-SA20 and ZSC-SA30, synthesised from ZSM-5 precursors with the initial Si/Al molar ratios of 20 and 30, respectively, show three well-resolved peaks indexed as (100), (110) and (200) reflections of an ordered 2D hexagonal structure with a p6mm symmetry, which is typical of SBA-15 type materials. Lowering the initial Si/Al ratio to 10 (ZSC-SA10) decreases the mesostructure ordering as confirmed by the only one visible reflection (100). However, when increasing the initial Si/Al ratio to 50, no reflections can be observed in the small angle range, suggesting the absence of an ordered mesostructure in this sample (ZSC-SA50). Wide angle XRD patterns (Figure 2) reveal the presence of a crystalline ZSM-5 phase in samples ZSC-SA30 and ZSC-SA50. Both materials show clear reflections in the 2θ regions of 8 - 10° and 23 - 25°, indicative of crystalline ZSM-5 zeolite. It should be noted that the reflections become sharper and more prominent with the increasing initial Si/Al ratio, suggesting a higher crystallinity degree in ZSC-SA50 compared to ZSC-SA30. For samples ZSC-SA10 and ZSC-SA20, there are no such reflections detected, implying a very low content or absence of a crystalline zeolite phase [12].

It has been reported that increasing the aluminum content of the initial gel mixture resulted in a decrease in the growth rate of ZSM-5 crystals from their precursors [13]. Accordingly, at the highest Si/Al ratio (the lowest aluminum content) the zeolite crystal growth is fast, consuming all precursor species; therefore, the mesoporous framework

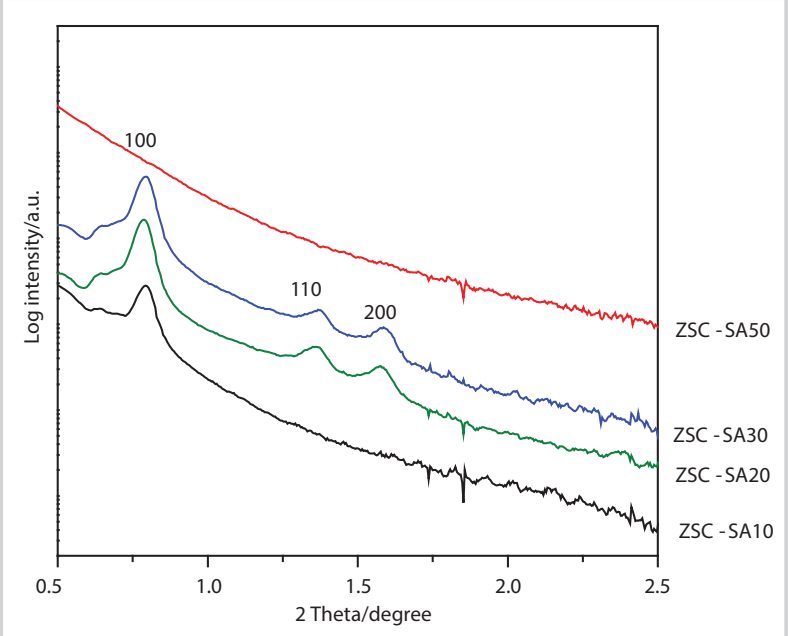

Figure 1. *SAXS patterns of ZSC catalysts with variable Si/Al ratios*

phase cannot be formed in sample ZSC-SA50. In contrast, using the lower initial Si/Al ratio (ZSC-SA10, ZSC-SA-20) produces ZSM-5 precursors which have been hardly consumed in the zeolite formation because of the slow zeolite growth. Consequently, the mesoporous

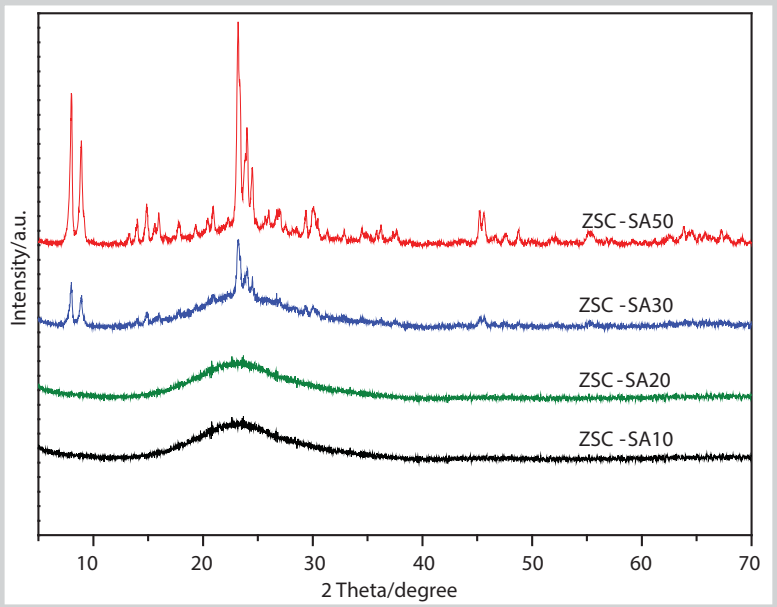

Figure 2. *XRD patterns of ZSC catalysts with variable Si/Al ratios*

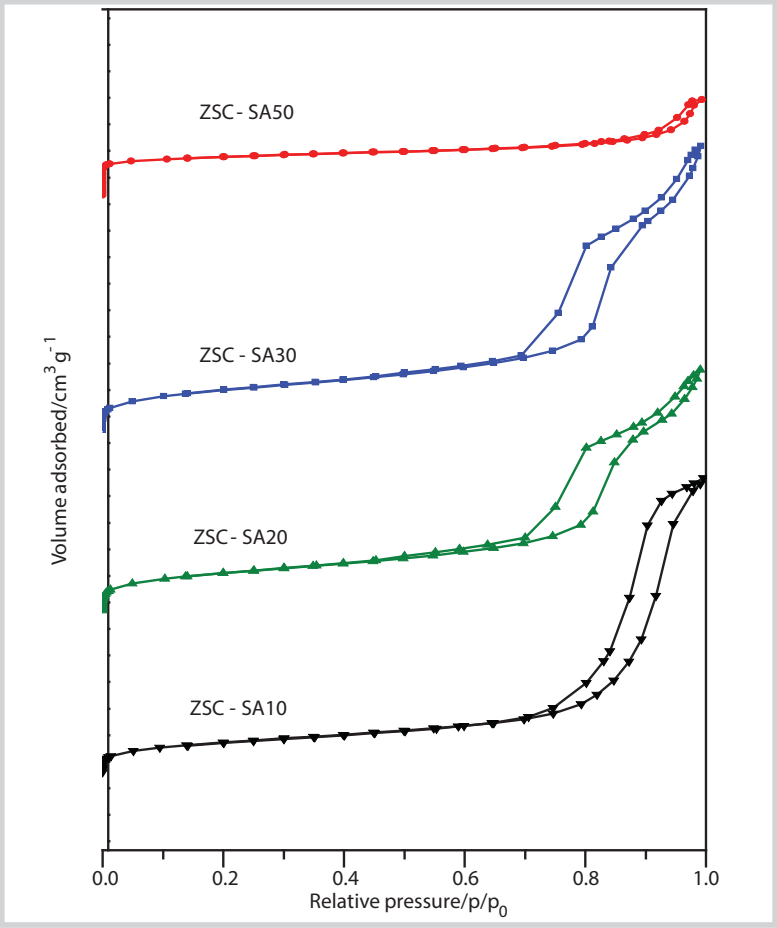

Figure 3. *Nitrogen sorption isotherms of ZSC catalysts with variable Si/Al ratios*

SBA-15 analog phase can be formed from these unreacted precursors in the second synthesis step. Notably, sample ZSC-SA30 contains sufficient amounts of ordered mesoporous SBA-15 analogs (Figure 1) and crystalline ZSM-5 (Figure 2), in order to form detectable amounts of ordered mesoporous phase and microporous zeolite phase.

The interpretation is further supported by the N_2 adsorption/desorption study. From the N_2 adsorption/desorption isotherms (Figure 3), one can see that samples ZSC-SA30, ZSC-SA20 and ZSC-SA10 possess type IV isotherms with a steep capillary condensation step in the relative pressure (p/p_0) range of 0.7 - 0.9, which is characteristic for an ordered mesostructure with a large and uniform pore size. However, the hysteresis loop of the isotherm of ZSC-SA10 is much less regular and shifts to higher relative pressures, suggesting that its pore uniformity is much degraded. It is noteworthy to mention that the isotherm of ZSC-SA30 shows a relatively steep increase of the adsorbed N_2 amount at low relative pressures ($p/p_0 < 0.01$), further confirming the presence of microporous crystalline ZSM-5 phase in this sample. The same phenomenon is observed from the isotherm of ZSC-SA50, but much more pronounced, which clearly evidences its microporous nature. Additionally, a high relative pressure uptake ($p/p_0 > 0.9$) occurs for all samples, suggesting the presence of nanoscale ZSM-5 phase and consequent inter-crystalline pores [12]. The detailed information about the textural properties of ZSC solids is listed in Table 1. The degraded porous structure of ZSC-SA10 is further affirmed by the lowest BET surface area of 210m^2/g compared to that of the other ZSC-SA samples (318 - 361m^2/g).

The local environment of the incorporated aluminum atoms in the representative ZSC samples was investigated by ^{27}Al MAS NMR spectroscopy (Figure 4). The ^{27}Al MAS NMR spectra of the studied samples exhibit two resonances centred at approximately 52ppm and ca. 3ppm which

Table 1. *Physicochemical properties of ZSC catalysts with variable Si/Al ratios*

Sample	Si/Al[a]	d_{100} (nm)	a_0 (nm)	D_p (nm)	S_{BET} (m^2/g)	V_t (cm^3/g)	Total acidity[b] (mmol NH_3/g)
ZSC-SA10	11	11.4	13.1	-	210	0.89	0.24
ZSC-SA20	18	11.2	12.9	9.1	323	0.96	0.30
ZSC-SA30	30	11.2	12.9	7.5	361	0.84	0.34
ZSC-SA50	48	-	-	-	318	0.24	0.27

[a]: In the final product analysed by AAS and ICP-AES; [b]: TPD-NH_3; d_{100}: Basal spacing; a_0: Unit cell parameter ($a_0 = 2 \times d_{100}/3^{1/2}$); D_p: Pore diameter; V_t: Total pore volume; the missing parameters are due to the absence of an ordered mesostructure.

are attributed to tetrahedrally and octahedrally co-ordinated aluminum, respectively. The fraction of octahedral aluminum increases at the expense of the tetrahedral aluminum when increasing the aluminum content in the initial gel mixture. In fact, ZSC-SA10 shows a major fraction of octahedral aluminum whereas ZSC-SA50 is dominated by tetrahedral aluminum. These results can be explained by considering the fact that before calcination, the aluminum atoms introduced by pH adjusting method are exclusively located as tetrahedrally co-ordinated aluminum species. The calcination causes the rearrangement of the aluminum co-ordination environment whose magnitude is strongly influenced by the density of aluminum sites [14, 15]. Thus, the samples with lower density of aluminum sites (ZSC-SA50 and ZSC-SA20) are more stable upon calcination, yielding the dominant fractions of tetrahedral aluminum. In contrast, sample ZSC-SA10 with the highest density of aluminum experiences a substantial conversion of tetrahedral aluminum to octahedral aluminum via condensation reactions between the neighbouring aluminum atoms, which resulted in a major fraction of octahedral aluminum.

The effect of the Si/Al ratio on the acidic properties was studied by temperature-programmed desorption of ammonia (NH_3-TPD). This method provides information on the number and strength of acid sites. The results are shown in Figure 5 and Table 1.

As shown in Figure 5, all samples display a similar TPD profile with two desorption peaks. The dominant peak at ca. 200°C corresponds to weak acid sites and the second broader peak in the range of 300 - 500°C arises from medium and strong acid sites. However, it should be stressed that the second desorption peak of ZSC-SA50 is

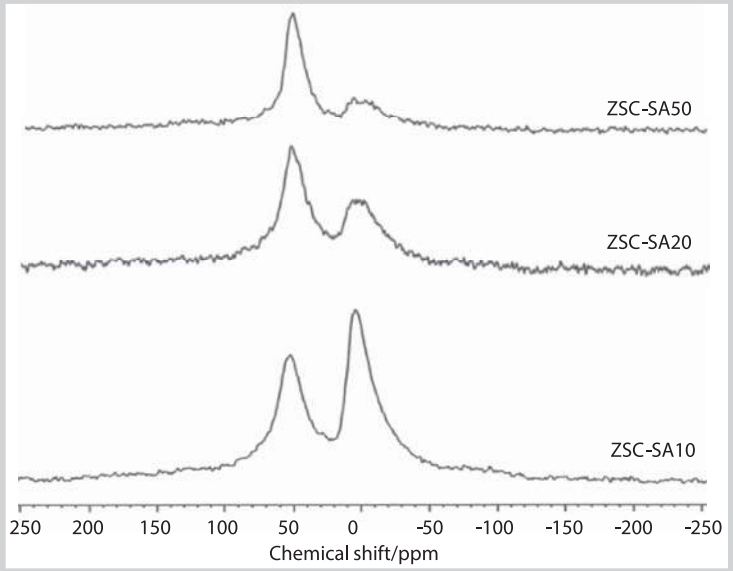

Figure 4. *^{27}Al NMR spectra of ZSC catalysts with variable Si/Al ratios*

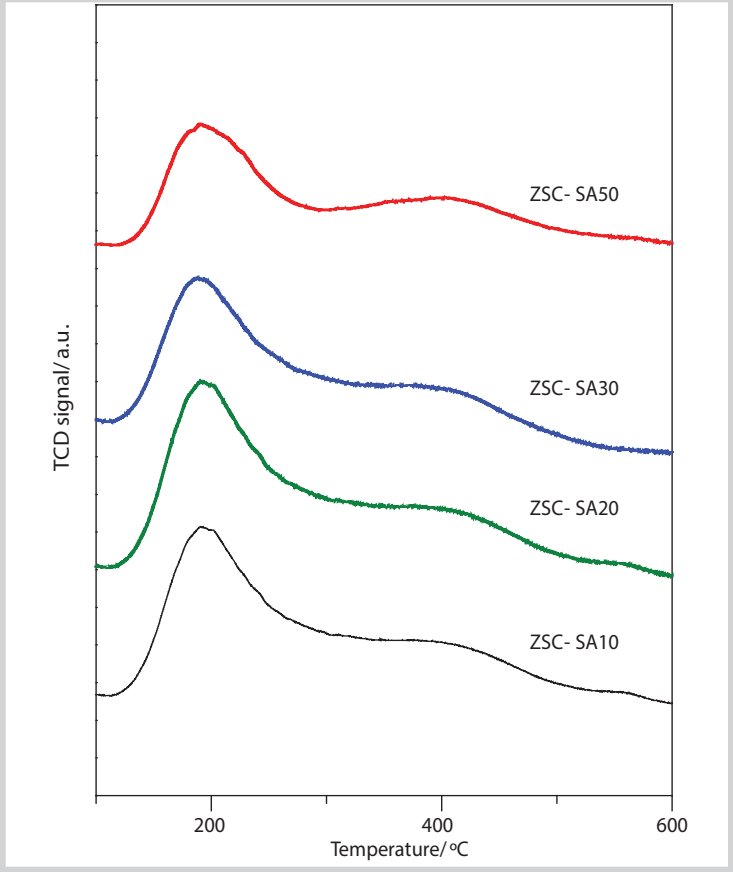

Figure 5. *NH_3-TPD profiles of ZSC catalysts with variable Si/Al ratios*

Table 2. *Catalytic performance of ZSC catalysts with variable Si/Al ratios in the catalytic cracking of waste cooking oil*

Catalysts	ZSC-SA10	ZSC-SA20	ZSC-SA30	ZSC-SA50
Conversion (wt%)	51.3	60.3	70.6	66.4
Product yields (wt%)				
Gas	16.6	21.1	30.7	25.2
Dry gas	2.2	2.4	2.6	1.6
LPG	9.6	13.5	22.1	18.1
Light olefins (C_2-C_4)	9.0	13.2	22.7	18.4
CO/CO_2	4.8	5.1	5.9	5.6
Gasoline	27.6	31.7	32.2	34.0
LCO	30.6	23.3	17.7	19.1
HCO	18.1	16.4	11.7	14.5
Coke	1.9	1.8	1.4	1.3
Water	5.2	5.7	6.3	5.9
Selectivity to C_2-C_4 olefins (%)	80.1	85.3	93.2	94.2

more obvious than that of the other samples, implying its higher fraction of strong acid sites. This might be the fact that ZSC-SA50 contains predominantly nanocrystalline ZSM-5 crystals which have strong Brønsted sites.

The number of acid sites estimated from the peak area in the TPD profiles is listed in Table 1. Although most of aluminum in the initial synthesis mixtures has been successfully incorporated in the final solids, the acid site amount decreases with increasing the incorporated aluminum for the first three samples: ZSC-SA30 > ZSC-SA20 > ZSC-SA10. It is acknowledged that the generation of acid sites from incorporated aluminum is heavily dependent on the crystallinity degree. For amorphous mesoporous SBA-15 type materials, only a partial fraction of grafted aluminum contributes to the formation of acid sites because of the lack of a long-range atomic order [16]. Using zeolite precursors as building blocks to construct a mesostructure has been proved to improve acidity thanks to the retention of zeolite building units in the mesoporous wall [12]. For crystalline zeolites, most of incorporated aluminum in the zeolite framework is tetrahedral aluminum which generates strong acid sites via bridging hydroxyl groups (Si-OH-Al) [17]. Thus, the higher amount of acid sites of ZSC-SA30 compared to that of ZSC-SA20 and ZSC-SA10 can be attributed to its higher content of crystalline ZSM-5 phase as shown by the XRD results (Figure 2) though the two latter samples have greater contents of incorporated aluminum. Similarly, the lowest acidity of ZSC-SA10 might be due to the fact that at such a low Si/Al ratio of 10, the crystallisation process occurs very slowly, resulting in little zeolite building units [13]. In addition, the highest incorporated aluminum content of this sample has caused the formation and aggregation of octahedrally co-ordinated aluminum species as confirmed by the NMR data which reduce the number of acid sites. On the other hand, it should be noted that sample ZSC-SA50 has a higher crystallinity but a lower acid amount than ZSC-SA30. One possible explanation is that ZSC-SA50 has the lowest incorporated aluminum in the framework (the highest Si/Al ratio) which has not been compensated by its highest crystallinity.

3.2. The performance of ZSC catalysts with variable Si/Al ratios in catalytic cracking of triglyceride-rich biomass

Catalytic cracking of triglyceride-rich biomass is often initiated by thermal decomposition of triglyceride molecules into fatty acids by means of free radical mechanism. Then the acid zeolite based catalyst controls the process and converts the formed fatty acid into oxygenated products mainly CO, CO_2 and water, and a mixture of hydrocarbons lumped into gaseous hydrocarbon, gasoline, light cycle (LCO) and heavy cycle oils (HCO) [1, 3, 9]. It is well known that the performance of a catalyst in the cracking of triglyceride-based feedstock is heavily influenced by its physicochemical properties, i.e. acidity and porosity. To understand such effect, in the present work the catalytic cracking of waste cooking oil (WCO) was performed over ZSC catalysts with the different Si/Al ratios under the optimised conditions, i.e. 550°C, a CTO mass ratio of 0.4 ($g \cdot g^{-1}$) and a reaction time of 12s [9]. The catalytic results are summarised in Table 2.

As the Si/Al ratio varies from 10 to 50, the conversion and product distribution over ZSC catalysts experience

significant changes because of their different total acidity and porosity. In fact, the conversion rises steadily from 51.3wt% (ZSC-SA10) to 70.6wt% (ZSC-SA30) as the Si/Al ratio increases from 10 to 30, corresponding to a relative increase of 37.6%. When the Si/Al ratio reaches 50, the conversion decreases to 66.4wt% (ZSC-SA50). In relation with the acid site amount, one can obtain a good correlation with the conversion, emphasising the important role of acid sites in the conversion of intermediate fatty acids to valuable hydrocarbons [7, 9].

Regarding the product distribution, it can be seen from Table 2 that ZSC-SA10 produces the least desirable products, i.e. gasoline (27.6wt%) and light olefins (9.0wt%), but the largest coke (1.9wt%). It sounds reasonable since this sample comprises predominant mesoporous SBA-15 analog phase with the lowest acid site amount. Thus, the large fraction of heavy products, i.e. HCO and LCO (ca. 48wt%) has not been converted to lighter and valuable products. On the other hand, the mesopore channels of SBA-15 analogs can facilitate the formation of polyaromatics involving cyclisation, aromatisation and condensation, leading to the increased formation of coke [9, 18]. A similar product distribution over ZSC-SA20 is obtained, reflecting its predominant SBA-15 analog phase. Furthermore, it should be noted that ZSC-SA20 shows higher yields of gasoline (31.7wt%) and light olefins (13.2wt%) than ZSC-SA10. This is because ZSC-SA20 possesses a greater acid site amount which is more effective than ZSC-SA10 in conversion of intermediate fatty acids to desired products, i.e. gasoline and light olefins.

Compared to the first two samples with the lower Si/Al ratios, ZSC-SA30 exhibits considerably higher yields of gasoline (32.2wt%) and light olefins (22.7wt%), but a lower yield of coke (1.4wt%). The superior catalytic performance of ZSC-SA30 primarily stems from the presence of substantial nano-ZSM-5 phase, which has been proved highly selective toward the formation of gasoline and light olefins [8, 9, 17, 18]. The shape selectivity generated by the medium pore zeolite ZSM-5 (pore mouths diameter of 0.52 - 0.56nm) preferentially directs the cracking process toward the formation of gasoline-range hydrocarbons and light olefins. At the same time, it severely suppresses the formation of polyaromatics because the limited space inside its medium pore channel cannot accommodate these intermediates, thereby reducing the coke fraction [17, 18].

With the predominant ZSM-5 phase, ZSC-SA50 displays a product distribution, which is very similar to that of ZSC-SA30. It is noteworthy that ZSC-SA50 produces more gasoline, but less light olefins than ZSC-SA30. The higher yield of gasoline over the former sample can be explained by the fact that this sample contains a higher content of nano-ZSM-5 phase as evidenced by the XRD results. However, the lower yield of light olefins over ZSC-SA50 can be assigned to its lower conversion. It appears logical since ZSC-SA50 and ZSC-SA30 have comparable selectivities of light olefins (94.2 and 93.2% respectively). Compared to that of ZSC-SA10 (80.1%) and ZSC-SA20 (85.3%), the superior selectivity of light olefins over ZSC-SA30 and ZSC-SA50 stresses the crucial role of substantial nano-ZSM-5 phase in improving the catalytic performance of ZSM-5 based catalysts in catalytic cracking of triglyceride-rich biomass.

4. Conclusions

We have shown that the Si/Al ratio in the initial synthesis mixture greatly influences the physicochemical properties and consequent catalytic performance of ZSC catalysts. Starting from ZSM-5 precursors with the lower Si/Al ratios, the resulting ZSC catalysts are predominated by SBA-15 analog phase (ZSC-SA10 and ZSC-SA20) while the high Si/Al ratio of 50 leads to the predominant nano-ZSM-5 phase (ZSC-SA50). Remarkably, sample ZSC-SA30 comprising the sufficient amount of nano ZSM-5 phase and SBA-15 analog phase detected by XRD and SAXS can be obtained from the ZSM-5 precursors with the initial Si/Al ratio of 30. The total acidity enhances as the Si/Al ratio increases because of the increased nano-ZSM-5 phase except ZSC-SA50. The high Si/Al ratio of 50 has resulted in the low incorporated aluminum, thus the reduced number of acid sites for ZSC-SA50. The catalytic cracking of waste cooking oil over ZSC catalysts with the variable Si/Al ratios evidences that the sufficient amount of nano-ZSM-5 phase obtained by properly adjusting the initial Si/Al ratio is required to achieve the superior catalytic performance of ZSC catalysts. These findings might stimulate future work on rational design of suitable ZSM-5 based catalysts for efficient conversion of triglyceride-rich biomass by petroleum technology to produce green gasoline and light olefins.

References

1. J.A.Melero, J.Iglesias, A.Garcia. *Biomass as renewable feedstock in standard refinery units. Feasibility, opportunities and challenges*. Energy Environmental Science. 2012; 5: p. 7393 - 7420.

2. G.W.Huber, A.Corma. *Synergies between bio- and oil refineries for the production of fuels from biomass*. Angewandte Chemie International Edition. 2007; 46(38): p. 7184 - 7201.

3. K.D.Maher, D.C.Bressler. *Pyrolysis of triglyceride materials for the production of renewable fuels and chemicals*. Bioresource Technology. 2007; 98(12): p. 2351 - 2368.

4. R.O.Idem, S.P.R.Katikaneni, N.N.Bakhshi. *Catalytic conversion of canola oil to fuels and chemicals: roles of catalyst acidity, basicity and shape selectivity on product distribution*. Fuel Processing Technology. 1997; 51(1, 2): p. 101 - 125.

5. D.Chen, N.I.Tracy, D.W.Crunkleton, G.L.Price. *Comparison of canola oil conversion over MFI, BEA, and FAU*. Applied Catalysis A: General. 2010; 384(1, 2): p. 206 - 212.

6. F.A.Twaiq, N.A.M.Zabidi, S.Bhatia. *Catalytic conversion of palm oil to hydrocarbons: performance of various zeolite catalysts*. Industrial Engineering Chemistry Research. 1999; 38(9): p. 3230 - 3237.

7. S.P.R.Katikaneni, J.D.Adjaye, R.O.Idem, N.N.Bakhshi. *Catalytic conversion of canola oil over potassium-impregnated HZSM-5 catalysts: C_2-C_4 olefin production and model reaction studies*. Industrial Engineering Chemistry Research. 1996; 35(10): p. 3332 - 3346.

8. J.A.Botas, D.P.Serrano, A.García, R.Ramos. *Catalytic conversion of rapeseed oil for the production of raw chemicals, fuels and carbon nanotubes over Ni-modified nanocrystalline and hierarchical ZSM-5*. Applied Catalysis B: Environmental. 2014; 145: p. 205 - 215.

9. Vu Xuan Hoan, Nguyen Sura, Dang Thanh Tung, Phan Minh Quoc Binh, Nguyen Anh Duc, U.Armbruster, A.Martin. *Catalytic cracking of triglyceride-rich biomass toward lower olefins over a Nano-ZSM-5/SBA-15 analog composite*. Catalysts. 2015; 5(4): p. 1692 - 1703.

10. Z.Nawaz, T.Xiaoping, F.Wei. *Influence of operating conditions, Si/Al ratio and doping of zinc on Pt-Sn/ZSM-5 catalyst for propane dehydrogenation to propene*. Korean Journal of Chemical Engineering. 2009; 26(6): p. 1528 - 1532.

11. X.Zhu, S.Liu, Y.Song, L.Xu. *Catalytic cracking of C_4 alkenes to propene and ethene: Influences of zeolites pore structures and Si/Al_2 ratios*. Applied Catalysis A: General. 2005; 288(1 - 2): p. 134 - 142.

12. Vu Xuan Hoan, U.Bentrup, M.Hunger, R.Kraehnert, U.Armbruster, A.Martin. *Direct synthesis of nanosized-ZSM-5/SBA-15 analog composites from preformed ZSM-5 precursors for improved catalytic performance as cracking catalyst*. Journal of Materials Science. 2014; 49(16): p. 5676 - 5689.

13. C.H.Cheng, G.Juttu, S.F.Mitchell, D.F.Shantz. *Synthesis, characterization and growth rates of aluminum- and Ge, Al-substituted silicalite-1 materials grown from clear solutions*. Journal Of Physical Chemistry B. 2006; 110(45): p. 22488 - 22495.

14. Q.Li, Z.Wu, B.Tu, S.S.Park, C.S.Ha, D.Zhao. *Highly hydrothermal stability of ordered mesoporous aluminosilicates Al-SBA-15 with high Si/Al ratio*. Microporous And Mesoporous Materials. 2010; 135(1 - 3): p. 95 - 104.

15. A.Ungureanu, B.Dragoi, V.Hulea, T.Cacciaguerra, D.Meloni, V.Solinas, E.Dumitriu. *Effect of aluminium incorporation by the "pH-adjusting" method on the structural, acidic and catalytic properties of mesoporous SBA-15*. Microporous and Mesoporous Material. 2012; 163: p. 51 - 64.

16. Z.Luan, J.A.Fournier. *In situ FTIR spectroscopic investigation of active sites and adsorbate interactions in mesoporous aluminosilicate SBA-15 molecular sieves*. Microporous and Mesoporous Material. 2005; 79(1 - 3): p. 235 - 240.

17. M.Stöcker. *Gas phase catalysis by zeolites*. Microporous and Mesoporous Material. 2005; 82(3): p. 257 - 292.

18. Vu Xuan Hoan, M.Schneider, U.Bentrup, Dang Thanh Tung, Phan Minh Quoc Binh, Nguyen Anh Duc, U.Armbruster, A.Martin. *Hierarchical ZSM-5 materials for an enhanced formation of gasoline-range hydrocarbons and light olefins in catalytic cracking of triglyceride-rich biomass*. Industrial and Engineering Chemistry Research. 2015; 54(6): p. 1773 - 1782.